Research on Engineering Structures & Materials
www.jresm.org
MIM Research Group

Research Article

Sustainable self-compacting concrete: A study on the combined effects of waste glass powder and metakaolin as cement replacements

Mutiu Adelodun Akinpelu[*,1,a], Abdullateef Olamilekan Amao[1,b], Ash-Shu'ara Marafa Salman[1,c], Daniel Sunday Gabriel[2,d]

[1]Department of Civil Engineering, Kwara State University, Malete, Kwara State, Nigeria
[2]*Department of Civil Engineering, University of Calgary, Canada*

Article Info

Article History:

Received 05 Jan 2025

Accepted 10 Mar 2025

Keywords:

Self-compacting concrete; *Waste glass powder;* Metakaolin; Microstructure

Abstract

Partial replacement of cement with eco-friendly pozzolanic materials, such as waste glass powder (WGP) and metakaolin (MK), offers a sustainable approach to improving the service life of self-compacting concrete (SCC). This study evaluates the effects of WGP and MK, individually (binary) and combined (ternary), as partial replacements for cement. Concrete mixes were assessed for workability, mechanical properties, and microstructure. Workability tests showed WGP enhances flow properties, while MK reduces them; however, their combined use at 15% replacement maintained performance. The ternary mix with 5% MK and 10% WGP (5MK+10WGP) exhibited superior mechanical properties, surpassing the control by 7.7% in compressive strength and 3.8% in split tensile strength at 56 days. SEM analysis revealed refined pores, reduced porosity, a denser microstructure, and well-formed C-S-H gels. XRD confirmed these findings with a pronounced broad hump in the 29°–34° 2θ range, indicative of well-developed C-S-H phases. This research demonstrates that incorporating 5MK+10WGP optimally balances workability, strength, and microstructure, providing a sustainable alternative for cementitious materials in SCC, reducing cement consumption, CO_2 emissions, and conserving natural resources.

1. Introduction

The construction industry has undergone substantial transformation since the advent of self-compacting concrete (SCC) [1]. A distinguishing feature of SCC is its ability to traverse heavily reinforced sections without requiring external vibration [2]. SCC flows effortlessly under its self-weight, filling molds of complex geometries while maintaining uniformity [3-5]. The adoption of SCC reduces reliance on vibratory tools and minimizes labor expenses [6, 7]. Over the past two decades, SCC has been a focal point of research globally [8].

However, despite its advantages, concrete remains prone to durability issues, which can lead to significant structural damage over time. Insufficient strength properties often result in cracks, reduced load-bearing capacity, and, in extreme cases, structural failure, necessitating costly repairs and maintenance. These defects have been linked to infrastructure deterioration and building collapses, particularly in regions where substandard materials are used. To mitigate these risks, researchers have emphasized the importance of optimizing concrete mix designs with alternative materials that enhance both mechanical strength and durability [9-12].

[*]Corresponding author: mutiu.akinpelu@kwasu.edu.ng
[a]orcid.org/0000-0003-4681-9874; [b]orcid.org/0009-0001-4157-0355; [c]orcid.org/0000-0001-8067-183X; [d]orcid.org/0009-0005-6522-4667
DOI: http://dx.doi.org/10.17515/resm2025-610ma0105rs

Concrete production also demands high energy consumption, leading to significant CO_2 emissions that contribute to environmental degradation [13]. This process exacerbates climate issues through the release of greenhouse gases [14-16]. Additionally, the continuous extraction of raw materials like aggregates, cement, and natural additives depletes natural resources, increasing costs over time [17]. The increasing depletion of natural resources has driven researchers in recent decades to explore alternative, sustainable materials for construction. One effective approach is the incorporation of waste materials into concrete, reducing dependence on virgin raw materials and mitigating environmental impact. Various waste materials, including recycled aggregates from demolished concrete, waste plastics, glass, rubber, tin scraps, by-product pozzolans, and agricultural or bio-wastes, have been investigated for their potential application in concrete production [18].

Among these alternatives, supplementary cementitious materials (SCMs) have gained significant attention for their ability to partially replace cement in mortar and concrete. Several researchers have explored SCMs derived from industrial by-products and agricultural residues [19-22]**.** Examples of commonly used SCMs include fly ash, silica fume, coffee silver skin, ground granulated blast furnace slag (GGBS), rice husk ash (RHA), and palm oil fuel ash. The incorporation of these materials has been shown to enhance the strength and durability of concrete while also serving as an indirect method of reducing CO_2 emissions into the atmosphere [6].

However, despite their advantages, the application of SCMs in Nigeria is hindered by their limited availability due to the country's low level of industrialization. This study aims to contribute to the growing body of research on sustainable concrete materials by exploring locally available alternatives that can enhance concrete performance while promoting environmental sustainability.

Glass is widely regarded as a vital material for infrastructural development. However, its global recycling rate remains significantly low. According to Statista [23], only around 1 out of 5 metric tonnes of glass produced globally were said to be recovered. Among this production, container glass accounts for 32%. In Nigeria, recycling rates for waste glass, as well as other materials like plastic and metal, are notably low due to inadequate infrastructure, the absence of formal recycling policies, and minimal engagement from manufacturers in waste recovery programmes [24]. These factors contribute to the growing accumulation of unrecycled glass, necessitating consistent management. Reusing waste glass to manufacture new products is often impractical due to variations in its chemical composition [25-27]. As a result, unrecycled glass is typically disposed of in landfills, where it decomposes extremely slowly [28]. Being chemically inert, glass remains non-biodegradable for over a million years when buried in soil [29]. This slow decomposition rate creates environmental challenges by taking up significant dumpsite space that could be utilised for biodegradable waste. The rising volume of global glass waste highlights the need for innovative methods to effectively utilise this material [1].

One promising approach suggested by researchers is incorporating waste glass into concrete production [30, 31]. Glass primarily consists of silica (SiO_2), although its composition may vary [32, 33]. Typically, pulverised glass (depending on its particle size) is used as a substitute for fine aggregates or cement in concrete mixes [30, 34]. When used in powdered form, glass can chemically interact with cement components during hydration, influencing the qualities of the resulting hardened concrete. However, the contribution of glass powder to the workability of SCC remains a subject of debate. Bisht et al. [34] and Tanwar et al. [35] recorded that blending of cement with glass waste negatively influenced the workability of the concrete. While others suggest improved workability in glass-modified mixes, often attributed to the smoothness as well as the sharp edges of the glass particles [36, 37].

Despite its potential, glass tends to react with the calcium hydroxide from cement hydration in a process known as alkali-silica reaction (ASR), leading to the formation of ASR gel, which subsequently absorbs water, causing expansion and cracking of the concrete [38-40]. However, studies have shown that the inclusion of SCMs like fly ash and metakaolin (MK) can mitigate ASR by reacting with calcium hydroxide from cement hydration to form additional hydrates. These hydrates refine the pore structure, reduce alkali availability, and enhance the overall properties of concrete [41].

Metakaolin (MK), a calcined product of kaolinite clay processed at 600–900°C [42, 43], is widely used in cement-based composites for its ability to enhance both mechanical and durability performance [44]; mitigate ASR expansion [41, 45]. However, MK reduces concrete fluidity and workability, requiring more water in the mix [46, 47]. Its strength gains are attributed to pozzolanic reactions with calcium hydroxide, enhanced hydration, and filler effects [48].

While many studies have explored the use of waste glass powder (WGP) and metakaolin (MK) as partial replacements for cement individually, their synergistic effects as a ternary blend in self-compacting concrete (SCC) remain largely underexplored. This research seeks to fill this gap by investigating the combined influence of MK and WGP on the flow and strength properties of SCC.

1.1. Research Significance

Recent research trends have increasingly focused on using supplementary cementitious materials (SCMs), such as metakaolin, silica fumes, rice husk ash and waste glass powder (WGP), in concrete to mitigate the environmental impacts of cement production [49-51]. Numerous studies have demonstrated that incorporating WGP into conventional concrete can significantly enhance both mechanical and durability properties. However, a major concern with the use of glass in concrete is its potential to trigger harmful alkali-silica reaction (ASR) expansion. To address this issue, research has shown that SCMs like fly ash and metakaolin can effectively mitigate ASR [52-54]. Despite these findings, the combined effect of WGP and metakaolin (MK) as a ternary blend on the rheology and strength properties of self-compacting concrete remains largely unexplored. Understanding the synergistic effect of ternary blended waste glass powder (WGP) and metakaolin (MK) as partial replacements for cement will contribute to environmental protection, enhance energy conservation, promote the production of sustainable concrete, and improve concrete performance across various applications.

2. Materials and Methods

2.1. Materials

The materials utilized in this study include; cement, fine aggregate (FA), coarse aggregate (CA), waste glass powder (WGP), metakaolin (MK), superplasticizer, and potable water. The details of the physical and particle distribution properties are further discussed in section 3.3 of this paper.

- Cement**:** Portland Limestone Cement of grade 42.5 (Dangote brand), sourced from a local retailer in Malete, Kwara State, Nigeria, was used in accordance with the requirements of BS EN197-1 [55]. Fine Aggregate (FA): Fine aggregate used in the study was river sand obtained from the Asa-dam River in Ilorin, which passed through a BS 4.75 mm sieve. The sand complies with the specifications of BS EN 12620 [56].
- Coarse Aggregate (CA): The coarse aggregate used was crushed granite with a maximum size of 9.6 mm, obtained from a local supplier in Ilorin. It was retained on a BS 4.75 mm sieve and met the requirements of BS EN 12620 [56].
- Waste Glass Powder (WGP): WGP was obtained from local aluminum glass window fabricators in Ilorin, processed into fine powdered passing through a BS 0.125 mm sieve. The characterization of WGP was conducted using X-ray Diffraction (XRD), X-ray Fluorescence (XRF), and Scanning Electron Microscopy (SEM) to analyze its crystallinity, oxide composition, and morphological properties.
- Metakaolin (MK): Commercially available metakaolin, sourced from the Nigeria Building and Road Research Institute (NBRRI) in Ota, Ogun State, was used. Similar to WGP, MK was characterized using XRD, XRF, and SEM to analyze its crystallinity, oxide composition, and morphology.
- Chemical Admixture: KONKRETO SP561, a superplasticizer purchased from PURECHEM MANUFACTURING LTD, was used as water reducing admixture.
- Water: Potable water sourced from the concrete laboratory at KWASU was used for both mixing and curing. It meets the requirements of BS EN 1008 [57].

2.2. Methods

2.2.1 Physical Property Test on Materials

The physical properties of cement, metakaolin, and waste glass—such as specific gravity, fineness, standard consistency, and initial and final setting times—were assessed in line with the standards outlined in BS EN197-1 [55]. Similarly, the physical characteristics of fine and coarse aggregates, including specific gravity, bulk density, particle size distribution (via sieve analysis), fineness modulus, and water absorption, were evaluated following the requirements of BS EN 1097-6 [58].

2.2.2 Mix Proportion, Mixing and Casting of SCC Specimens

The mix design procedure adopted for this study was based on the EFNARC [59], [60] provisions, with some modifications since there is no standardized mix design procedure for SCC. Multiple trial mixes were performed in the laboratory to identify the optimal proportions that would ensure SCC with no segregation or bleeding while satisfying both fresh and hardened state performance criteria. In total, 22 SCC mix designs were developed for this research, their mix contents and labels are presented in Table 1.

Table 1. Concrete mix proportion

S/N	Mix Label	Cement (kg)	MK (kg)	WGP (kg)	Sand (kg)	Granite (kg)	Water (kg)	SP (ml)
1	Control	4.6	0.0	0.0	9.2	6.1	2.3	69.0
2	5MK	4.4	0.2	0.0	9.2	6.1	2.3	92.0
3	10MK	4.2	0.5	0.0	9.2	6.1	2.3	92.0
4	15MK	3.9	0.7	0.0	9.2	6.1	2.3	92.0
5	20MK	3.7	0.9	0.0	9.2	6.1	2.3	92.0
6	25MK	3.5	1.2	0.0	9.2	6.1	2.3	92.0
7	30MK	3.2	1.4	0.0	9.2	6.1	2.3	92.0
8	5WG	4.4	0.0	0.2	9.2	6.1	2.3	69.0
9	10WG	4.2	0.0	0.5	9.2	6.1	2.3	69.0
10	15 WG	3.9	0.0	0.7	9.2	6.1	2.3	69.0
11	20 WG	3.7	0.0	0.9	9.2	6.1	2.3	69.0
12	25 WG	3.5	0.0	1.2	9.2	6.1	2.3	69.0
13	30 WG	3.2	0.0	1.4	9.2	6.1	2.3	69.0
14	5Mk5WG	4.2	0.2	0.2	9.2	6.1	2.3	69.0
15	5MK10WG	3.9	0.2	0.5	9.2	6.1	2.3	69.0
16	5MK15WG	3.7	0.2	0.7	9.2	6.1	2.3	69.0
17	10Mk5WG	3.9	0.5	0.2	9.2	6.1	2.3	69.0
18	10MK10WG	3.7	0.5	0.5	9.2	6.1	2.3	69.0
19	10MK15WG	3.5	0.5	0.7	9.2	6.1	2.3	69.0
20	15Mk5WG	3.7	0.7	0.2	9.2	6.1	2.3	69.0
21	15MK10WG	3.5	0.7	0.5	9.2	6.1	2.3	69.0
22	15MK15WG	3.2	0.7	0.7	9.2	6.1	2.3	69.0

EFNARC [59] limits the cement content in SCC to 500 kg/m^3 to control temperature rise and thermal shrinkage cracking, while the total powder content ranges between 380–600 kg/m^3. For this design, the cement content was maintained at the maximum value of 500 kg/m^3 since no other powder was included in the control mix. The water–cement ratio was maintained at 0.5, as this falls within the acceptable limit, resulting in 250 kg of water per cubic meter of concrete.

The total aggregate weight of 1650 kg/m^3 was obtained by subtracting the weight of cement and water from the unit weight of concrete (i.e., 2400 – 500 – 250). To achieve the required workability in the fresh state, the sand fraction was increased from the recommended 55% to 60% of the total aggregate volume, while the remaining 40% constituted the coarse aggregate (crushed granite) fraction. The superplasticizer dosage was based on the manufacturer's guidelines, which recommend a maximum of 2 liters per 100 kg of cement. The applied dosage ranged between 1.5 to 2 liters per 100 kg of cement. Typical mix design details for 0.03 m^3 of SCC, as adopted in the study, are presented in Table 1.

A laboratory drum mixer was used for blending the materials. Initially, dry ingredients including cement, metakaolin, waste glass powder, fine aggregate, and coarse aggregate were measured according to the mix design and added to the drum mixer. The mixing process was carried out in three stages: (1) the dry materials were mixed for 60 seconds, (2) 50% of the water was added and mixed till a homogenous mix is achieved, and (3) the remaining water and superplasticizer were incorporated, followed by two additional minutes of mixing. Fresh concrete tests, including slump flow, V-funnel, and L-box tests, were conducted immediately after mixing to ensure adherence to EFNARC [60] standards. The concrete was then placed into cleaned and oiled molds and allowed to set for 24 hours. A total of 396 samples were produced, comprising 198 cubes (100 × 100 × 100 mm) and 198 cylinders (100 mm Ø × 200 mm height). After a day, the concrete specimens were demolded and submerged in water for curing. Compressive strength and split tensile strength tests were carried out at 7, 28, and 56 days.

2.2.4 Fresh Property Tests of Concrete

To evaluate the workability of self-compacting concrete (SCC), several tests were conducted as follows:

2.4.2.1 Slump Flow and T_{50cm} Slump Flow

The filling ability of SCC containing waste glass and metakaolin was assessed through the slump flow and T_{50cm} tests as shown in Fig. 1. Concrete was poured into a standard slump cone, and the resulting flow diameter was measured. Additionally, the time taken for the concrete to spread to a 50cm diameter (T_{50cm}) was recorded. These tests were conducted in accordance with BS EN 12350-2 [61].

Fig. 1. Slump flow testing of the fresh concrete

2.2.4.2 V-Funnel and V-Funnel at 5 Minutes

The V-funnel test was performed to determine the flowability and viscosity of the SCC. The time taken for the concrete to flow through a funnel-shaped mold (see Fig. 2) was measured both immediately after mixing and after a 5-minute delay to evaluate any changes in flow characteristics over time. This test complied with BS EN 12350-9 [62].

Fig. 2. V-Funnel tests on fresh concrete

2.2.4.3 L-Box Test

The passing ability of the SCC was measured using the L-box test shown in Fig.3 . Concrete was poured into an L-shaped mold, and the ratio of the concrete height in the horizontal section to that in the vertical section was calculated. This ratio indicates the concrete's ability to flow through narrow spaces and around obstacles. The test adhered to BS EN 12350-10 [63].

Fig.3. L-Box test

2.2.5 Concrete Hardened Property Tests

2.2.5.1 Compressive Strength Test

Compressive strength tests were performed on three 100mm cube specimens for each mix at curing ages of 7, 28, and 56 days, following BS EN 12390-3 [64] guidelines. Concrete samples were prepared using the mix proportions detailed in Table 1. The compressive strength (f_c) of the specimens containing waste glass powder and metakaolin was calculated by dividing the maximum load at failure (Pmax) by the cross-sectional area of the cube. The load was applied at a rate of 0.5 MPa/s using a compressive testing machine.

2.2.5.2 Split Tensile Strength test

Split tensile strength tests were performed on three cylindrical specimens with dimensions of 100mm diameter and 200mm height for each mix, conforming to BS EN 12390-6 [65]. A diametral load was applied at a rate of 0.05 MPa/s using a compression testing machine. The splitting tensile strength (f_{st}) of the concrete containing waste glass powder and metakaolin was calculated using the formula:

$$f_{st} = \frac{2P_{max}}{\pi LD} \quad (1)$$

where: P_{max} is the maximum load at failure, L is the length of the cylinder, and D is its diameter.

(a)

(b)

Fig. 4. Compressive and tensile strenght test on hardened concrete specimen (a) Compressive and (b) Tensile

2.2.6 Microstructural Analysis of Concrete Specimen

2.2.6.1 Scanning Electron Microscopy (SEM) Test for Concrete Specimen

Concrete specimens were prepared for SEM analysis by collecting chunks from SCC cube samples tested after 28 days cutting them into smaller pieces (Fig. 5), embedding in epoxy resin, polishing with silicon carbide paper, mounting on aluminum stubs, and coating with layer of carbon to enable high-resolution imaging of the concrete microstructure.

Fig. 5. Sample preparation for SEM analysis

3.2.6.2 X-Ray Diffraction (XRD) Test for Concrete Specimen

Concrete specimens were prepared for XRD analysis by further crushing the cube samples tested after 28 days into smaller fragment using mortar and pestle. The fragments were then grounded into fine powder using grinder to ensure uniform particle size. The powder was subsequently sieved through a 63micromes sieve to remove any other larger particles, and then stored in an airtight container shown in Fig. 6 to prevent moisture absorption. The powdered samples were analyzed at the National Steel Raw Materials Exploration Agency, Kaduna State, where EMPYREAN DIFFRACTOMETER was used for the analysis.

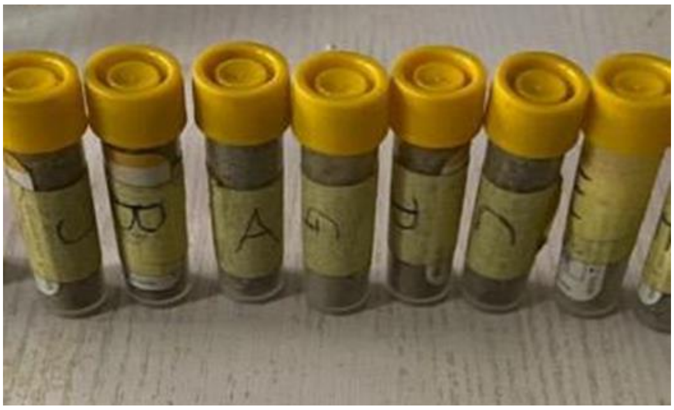

Fig. 6. Powdered concrete specimen prepared for XRD analysis

3. Results and Discussion

3.1 Physical Properties of Used Materials

Table 2 presents the outcomes of the physical properties tests conducted on the binder materials, including cement, waste glass, and metakaolin. The evaluated properties cover specific gravity, standard consistency, fineness, as well as the initial and final setting times. The findings indicate that all binder materials comply with the requirements specified for SCC binder ingredients, as outlined in BS EN197-1 [55]. Similarly, the physical properties of fine and coarse aggregates, such as water absorption, fineness modulus specific gravity and bulk density are detailed in Table 2. The findings indicate that these aggregates comply with the recommended ranges for SCC production, as specified in BS EN 1097-6 [58].

Table 2. Physical properties of used materials

Property	Cement	Waste glass powder	Metakaolin	Fine aggregate	Coarse aggregate
Specific gravity	3.1	2.4	2.6	2.60	2.72
Consistency (%)	29	-	-	-	-
Fineness test (%)	2.93	64.19	46.3	-	-
Initial setting time	120	-	-	-	-
Final setting time	360	-	-	-	-
Fineness modulus	-	-	-	2.70	5.97
Water absorption	-	-	-	2.20	0.80
Bulk density(kg/m^3)	-	-	-	1585	1679

The particle size distribution curves for fine and coarse aggregates, shown in Fig. 7, provide critical parameters for assessing gradation. For fine aggregate, the coefficient of curvature (1.03) falls within the range recommended by [66], while the coefficient of uniformity (2.7) is slightly below the standard range, classifying the fine aggregate as well graded. For coarse aggregate, both the coefficient of curvature (1.2) and coefficient of uniformity (4.1) lie within the recommended ranges of ASTM C1602/C1602M [66], classifying it as well graded. These gradation characteristics indicate the suitability of both aggregates for use in SCC.

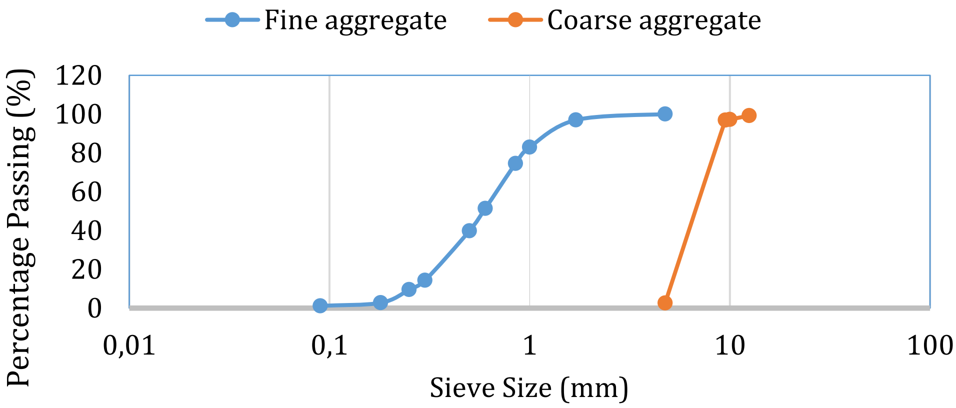

Fig. 7. Particle size distribution graph of fine and coarse aggregate

3.2 Characterization of Waste Glass and Metakaolin

The XRD diffractogram offers valuable insights into the crystalline or amorphous nature of waste glass powder and metakaolin. Fig. 8 displays the diffractograms plotted for these materials, revealing that the majority of waste glass powder and metakaolin exist in an amorphous state, with distinct Quartz (SiO2) crystals evident at certain sharp peaks. The broad hump observed in the graphs of both materials indicates their amorphous characteristics, qualifying them as pozzolanic materials. In addition, the result of the XRF showing the chemical and oxide composition of waste glass and metakaolin are presented in Table 3. The result shows a slightly lower (SiO_2 + Al_2O_3 +Fe_2O_3 (%) than ASTM C618 recommended percentage for both MK and WGP.

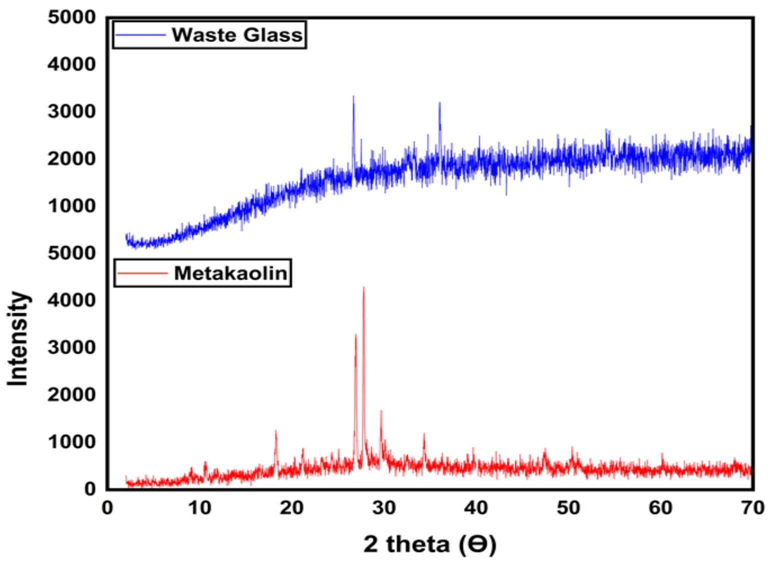

Fig. 8. XRD of materials characterization

Table 3. Chemical composition of Cement, Metakaolin and Waste glass powder (XRF results)

Composition (%)	Cement	Waste glass powder	Metakaolin
SiO_2	20.62	64.6	42.5
Fe_2O_3	3.07	1.4	9.3
Al_2O_3	5.35	2.7	15.2
SO_3(≤ 4)	-	0.1	0.5
SiO_2 + Al_2O_3 +Fe_2O_3(≥70%)		68.8	67

SEM image shows the micrograph of WG and MK at the magnification of 250. Fig. 8a and 8b shows micrograph for WGP and MK respectively. Fig. 8a shows that waste glass powder has angular irregular shape particles with smoother surfaces that are loosely packed together. Fig. 3b shows that metakaolin have particles that are closely packed with little micropores. The particles are irregular with rough surfaces and high surfaces area.

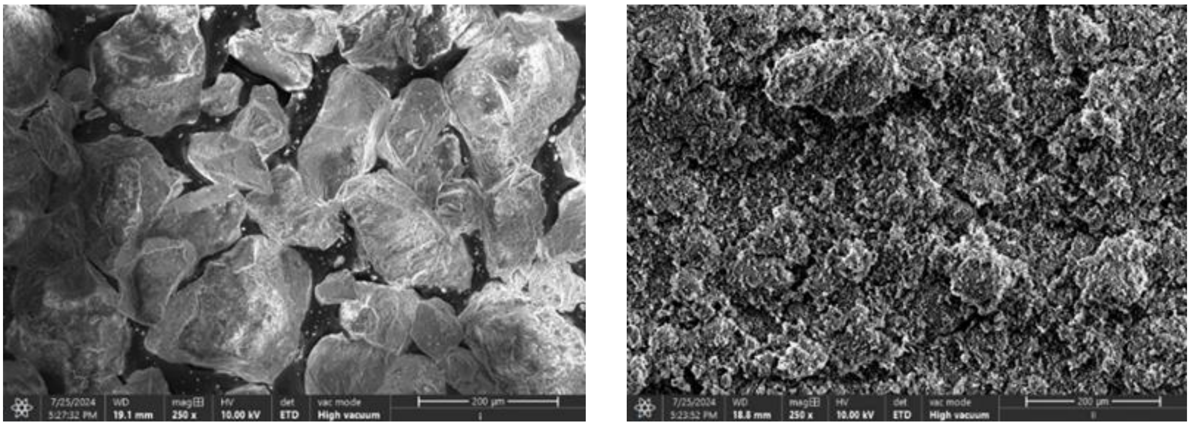

(a) (b)

Fig. 8. (a) SEM image for waste glass powder, and (b) SEM image for Metakaolin

3.3 Fresh Properties of Concrete

3.3.1 Slump Flow and T_{50cm} Slump flow

The effects of binary blends of WGP and MK with cement, as well as the ternary combination of WGP+MK with cement, on the slump flow diameter and T_{50cm} flow time are illustrated in Fig. 9. The results reveal that increasing the MK content decreases the slump flow diameter while increasing the T_{50cm} flow time, thereby reducing the overall flowability. In contrast, WGP exhibits improved slump flow diameters, and reduced T_{50cm} flow times compared to both MK and the control mix, indicating enhanced flowability. However, a reduction in flow diameter is observed when the replacement level exceeds 10%. This observation is consistent with findings by Guignone et al. [69].

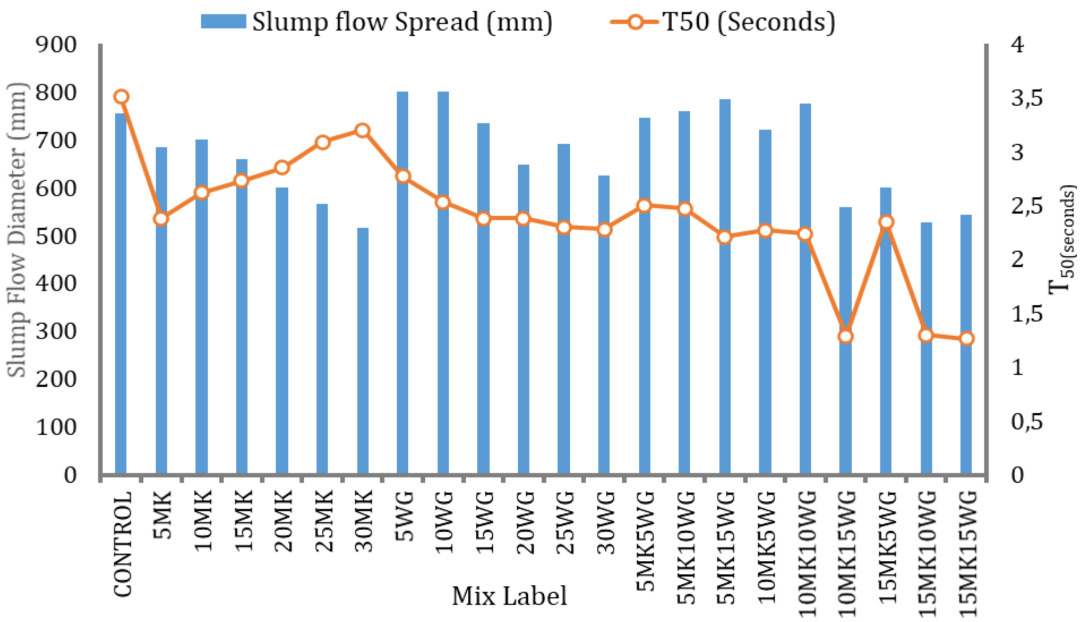

Fig. 9. Slump flow diameter and T50cm Slump flow of the SCC mixes

The ternary blend demonstrates improved slump flow diameters and lower T_{50cm} flow times at replacement levels of up to 20%, signifying better flowability. However, beyond the 20% replacement level, both the slump flow diameter and T_{50cm} flow times fall below the EFNARC [60] recommended range for flowability.

3.3.2 V-funnel and V-funnel @$T_{5minute}$

The low workability beyond 20% for the ternary blended mixtures could be due to increased surface area, higher water demand, and reduced cementitious content. The fine particles of glass powder and metakaolin absorb more water, leaving less free water for flow, while excessive replacement reduces the cement content, weakening paste cohesion. Additionally, the optimal particle packing effect diminishes at high replacement levels, leading to a stiffer mix with lower flowability.

The segregation resistance of SCC is evaluated using a V-funnel, which measures the time required for concrete to flow through a V-shaped funnel. The results presented in Fig. 10 indicate that the V-funnel flow time (Vf) for the concrete mixtures ranges between 5.6s and 7.17s, aligning with the recommended EFNARC limits, except for certain outliers among the ternary mixes. The data reveals that incorporating WGP enhances the flow properties of the mix, resulting in reduced flow times, whereas MK has the opposite effect, increasing the flow time by reducing the concrete's fluidity.

For $T_{5minutes}$, the flow times for MK and WGP mixes range between 6.26s and 9.55s, remaining within the EFNARC [60] recommended limits. Specifically, the inclusion of WGP consistently reduces $T_{5minutes}$ flow times, ranging from 8.66s at 5% WGP to 7.83s at 30% WGP. However, the flow times for MK-blended mixtures show erratic behaviour, with the 30% MK mix recording the highest $T_{5minutes}$ flow time of 9.55s, confirming MK's negative impact on concrete flow. The incorporation of WGP as part of a ternary blend with MK mitigates this effect, improving the flow time of MK-blended mixtures.

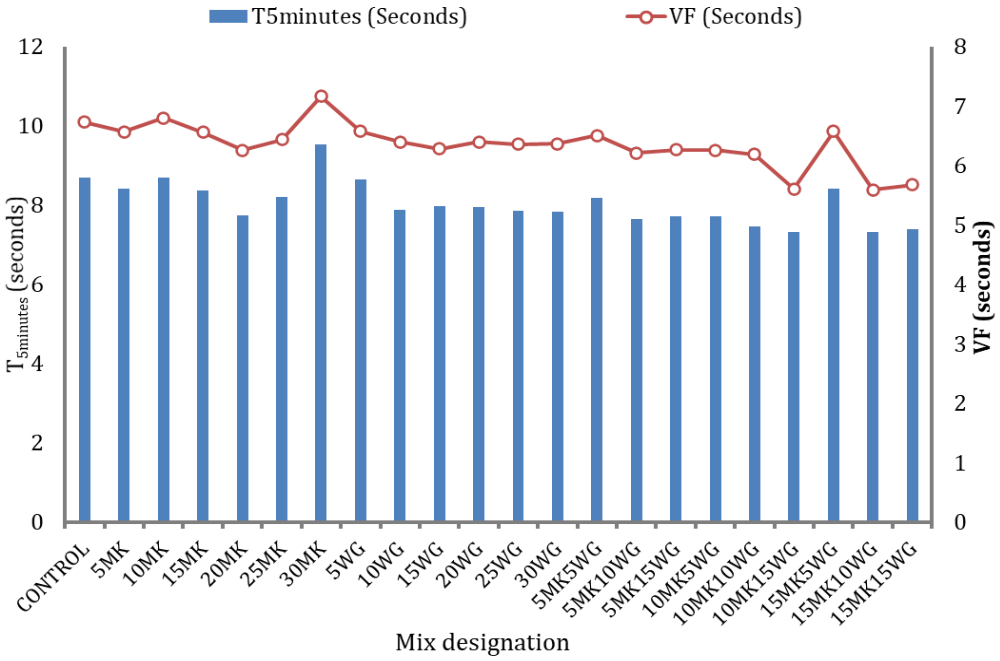

Fig. 10. V-funnel and V-funnel @ $T_{5minutes}$ of the SCC mixes

3.3.3 L- Box Result

The results of the L-box test, presented in Fig. 11, evaluate the ability of SCC to flow through and fill narrow spaces while navigating around obstacles. The blocking ratio, which represents the ability of SCC to pass through obstacles without segregation, is computed as the ratio of the final concrete height at the end of the L-box test to the initial height. This metric is crucial in evaluating the passing ability of SCC, ensuring that the mix can flow smoothly through reinforcement without blockage. The findings indicate that the blocking ratio for all binary mixes of MK and WGP ranges between 0.81 and 1, meeting the EFNARC [60] recommended values for the L-box test. Notably, the binary mixture of WGP and cement, up to a 10% replacement level, exhibits the highest blocking ratio, demonstrating superior passing ability. However, for the ternary combination, the blocking ratio drops below the recommended range when the replacement level exceeds 20%.

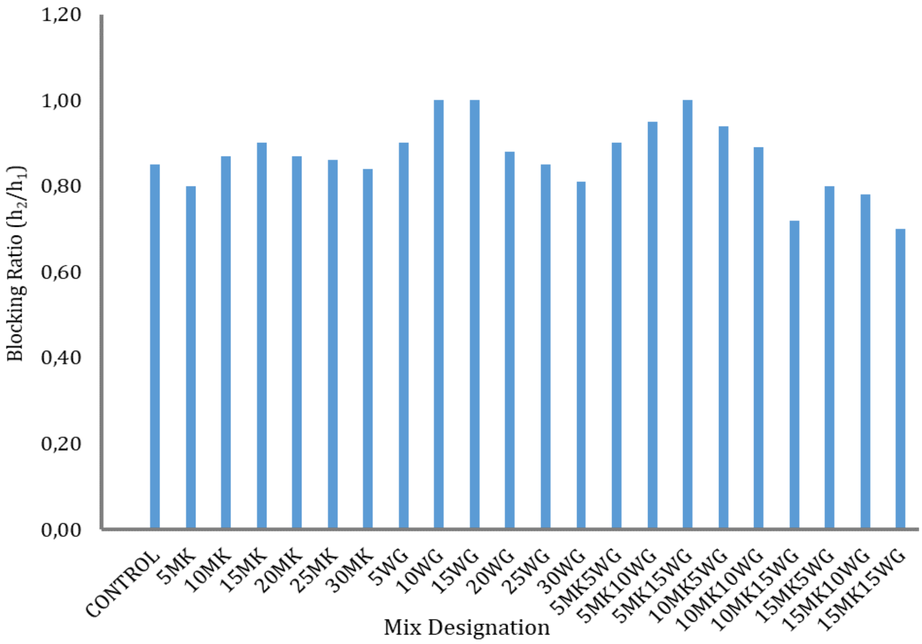

Fig. 11. L- box tests results to determine the passing ability SCC mixes

3.4 Hardened Properties of Concrete

3.4.1 Compressive Strength

The experimental results for the compressive strength of concrete samples with varying percentages of binary and ternary combinations of MK and WGP with cement are presented in Figures 12, 14, and 17. The binary blend of MK with cement, shown in Fig. 12, demonstrates that compressive strength improves with increasing MK content, reaching its peak at 15% replacement across all curing ages. This observation aligns with the findings of Chavali et al. [70] and Ofuyatan et al. [71], who identified 15% MK replacement as the optimum level for enhancing the compressive strength of concrete compared to the control mix.

At 7 days, 10MK and 15MK mixes were able to achieve strength similar to or slightly greater than the control. The improvement in compressive strength at 7 days with metakaolin (MK) replacement is primarily due to hydration acceleration and filler effects, with minimal pozzolanic contribution at this stage. MK's fine particle size and high surface area enhance nucleation, accelerating the formation of hydration products like calcium silicate hydrate (C-S-H) and boosting early-age strength. Its filler effect reduces voids, improves packing density, and refines the microstructure, further contributing to strength. While the pozzolanic reaction between MK and calcium hydroxide ($Ca(OH)_2$) begins during this period, its impact remains limited, as significant pozzolanic activity typically develops after 7 days. Beyond 15% replacement, the dilution effect becomes significant. The amount of cement available for hydration decreases, resulting in less primary C-S-H formation.

At 56 days, only the 15% metakaolin (MK) replacement surpasses the control strength, while 5% and 10% replacements show improvements but do not exceed it. This is due to the optimal balance at 15%, where pozzolanic activity and hydration synergize to produce additional calcium silicate hydrate (C-S-H), significantly densifying the matrix. At lower replacements, MK enhances the microstructure and contributes moderately through pozzolanic reactions, but the cement content remains dominant, limiting the overall strength gain. Higher replacements dilute the cement content, reducing hydration products and leaving unreacted MK, which acts as an inert material. Thus, 15% MK replacement provides the best long-term performance by maximizing both hydration and pozzolanic contributions. A similar observation was reported by Lekhya and Kumar [72] on the utilisation of silica fume (SF) in high-performance concrete, where they noted that a 15% replacement exhibited compressive strength surpassing the control mixes at both 28 and 90 days. Almari et al. [73] also observed a 3.13% increase in compressive strength at 28 days due to a ternary blend of cement, 10% fly ash, and silica (25 kg/m^3), whereas a combination of cement, 15% metakaolin, and silica (25 kg/m^3) enhanced strength by 4.1%.

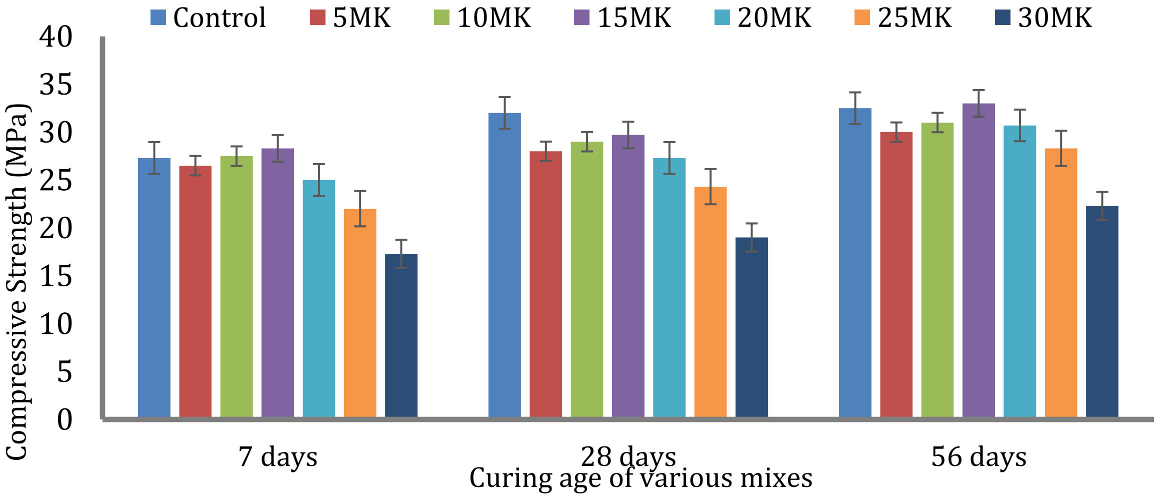

Fig. 12. Compressive strength tests result of binary blended MK with cement

The microstructural evolution of the hardened concrete samples at 56 days observed with increasing MK replacement levels is illustrated in the SEM images (Figs. 13a, 13b, and 13c). Fig. 13a (control sample) shows visible porosity and some unreacted cement particles but maintains a relatively uniform microstructure. This uniformity supports adequate hydration and structural stability. Fig. 13b reveals disrupted microstructure due to incomplete pozzolanic reactions between MK and calcium hydroxide, resulting in a less cohesive matrix. Fig. 13c, corresponding to 15% MK replacement, shows a denser and more refined microstructure with reduced porosity and improved particle packing, which likely contributes to the enhanced strength observed in mechanical tests.

The XRD patterns, presented in Fig. 14, confirm the hydration products of the hardened concrete samples. The 15% MK sample shows broader humps rather than sharp peaks in the 27°–35° 2θ range, with a noticeable intensity around 29.3° 2θ, indicating the presence of calcium silicate hydrate (C-S-H), the primary strength-giving phase. Additionally, the 15% MK sample exhibits other hydration products such as portlandite ($Ca(OH)_2$) and ettringite.

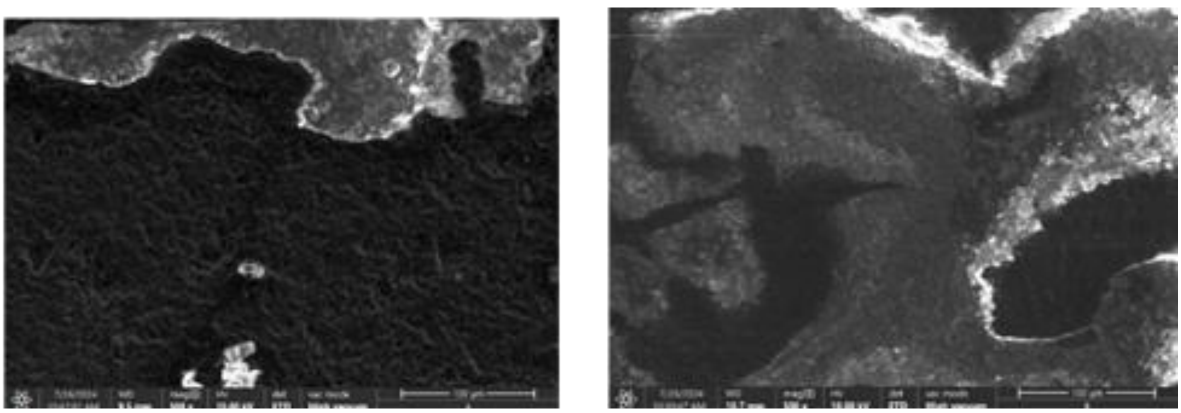

(a) (b)

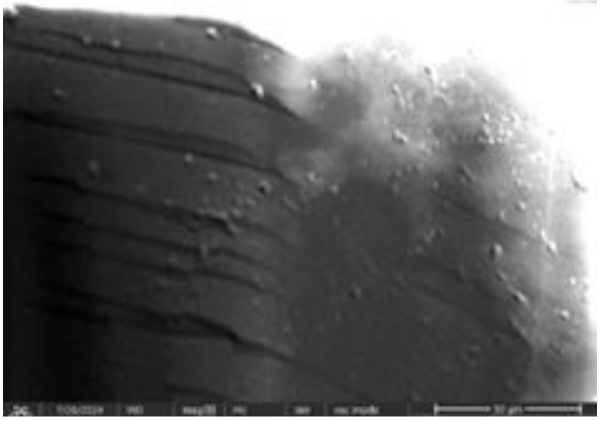

(c)

Fig 13. (a)SEM image control, (b) SEM image of 5MK, and (c) SEM image of 15MK

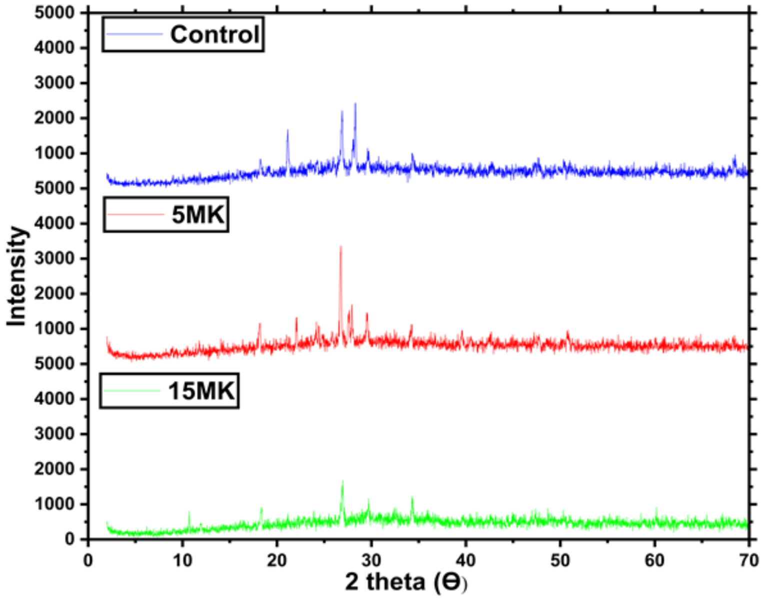

Fig. 14. XRD Comparison of various Metakaolin replacements

This more complete hydration, compared to the control (0% MK) and 5% MK samples, leads to a denser microstructure, which correlates with the improved compressive strength observed in the 15% MK mix. The enhanced C-S-H formation contributes significantly to the increased strength, supporting the role of MK in improving the mechanical properties of concrete. Fig. 15. shows a similar trend for the binary blend of WGP with cement as observed with MK, where the compressive strength increases with increasing WGP content up to 15% replacement. Beyond this point, further increases in WGP replacement led to a reduction in strength. This slightly exceeds the 10% optimum replacement level reported by Fonchou et al. [74] and Shamsudeen et al. [75].

The microstructural characteristics observed with 5% and 15% replacement of cement with WGP, relative to the control, are illustrated in the SEM images (Figs. 16a, 16b, and 16c). Fig. 16b reveals a modest enhancement in the microstructure due to the pozzolanic reaction of WGP, though the strength remains slightly below that of the control. In contrast, Fig. 16c exhibits a significantly denser and more refined microstructure, characterized by reduced porosity and increased formation of C-S-H gels. This improved microstructure underpins the superior strength achieved at the 15% replacement level compared to both the control and the 5% replacement.

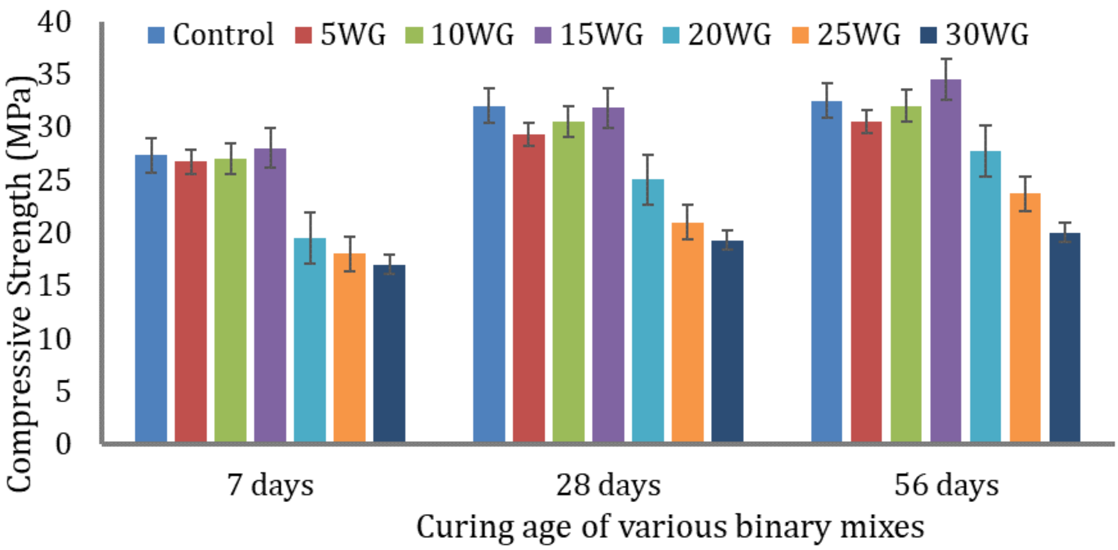

Fig. 15. Compressive strength tests result of binary blended WGP with cement

The XRD patterns of the hardened binary blends of WGP and cement for the control, 5% replacement, and 15% replacement levels are shown in Fig. 17 The 5% replacement sample exhibits a reduction in the intensity of crystalline peaks, such as portlandite, alongside a subtle broad hump, suggesting the onset of C-S-H formation. In contrast, the 15% replacement sample displays a more pronounced broad hump within the 27°–35° 2θ range, indicating more extensive or complete C-S-H formation. The reduction in crystalline peaks compared to the control signifies increased pozzolanic activity, which contributes to a denser microstructure and the higher strength observed in the sample with 15% WGP replacement.

The ternary mix 5MK+10WGP, as shown in Fig. 18, achieved the highest compressive strength among all tested concrete mixes, establishing it as the optimum replacement level. However, its early-age compressive strength was lower than that of the control mix. This behaviour aligns with findings by Guignone et al. [69], who reported that ternary blends of WGP and MK with cement could support up to 20% replacement while maintaining compressive strength.

The reduced early-age strength may be attributed to the slow nature of pozzolanic or secondary hydration reactions. These reactions depend on the availability of calcium hydroxide (CH) released during primary hydration of the cement and its interaction with amorphous silica from the pozzolans, processes which inherently progress at a slower rate [76]. However, the ternary mix of ultrafine silica fume (UFFA) and fly ash at 10% and 15% replacement (a total of 25%) in HPC achieved higher replacement level, exhibiting a significant improvement in compressive strength of around 12% at 90 days due to the extended pozzolanic reaction of SF and UFFA [72].

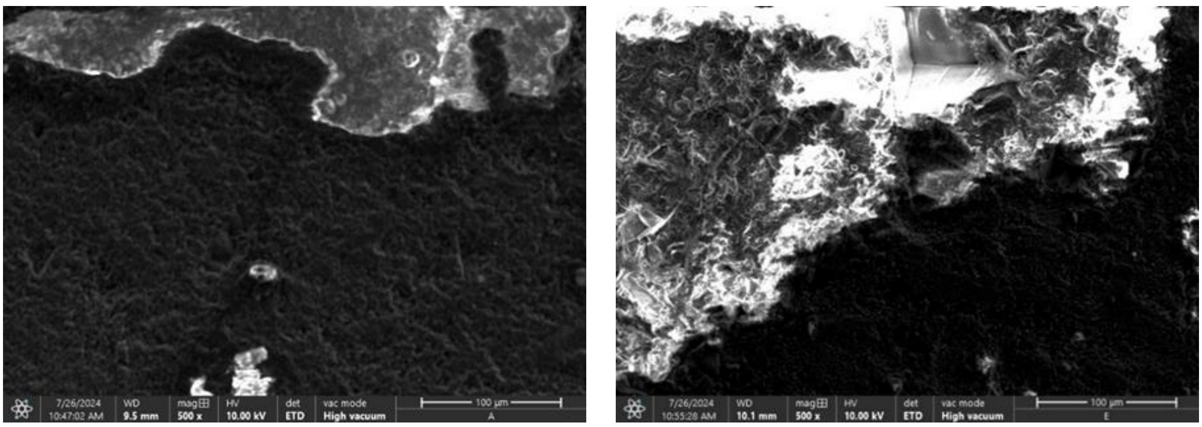

(a) (b)

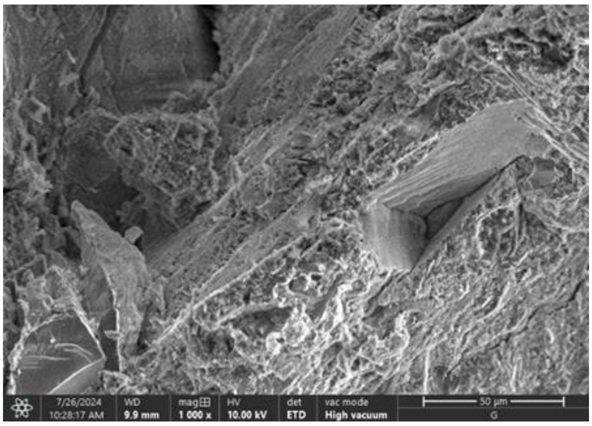

(c)

Fig 16. (a) SEM image of control, (b) SEM image of 5WGP, and (c) SEM image of 15WGP

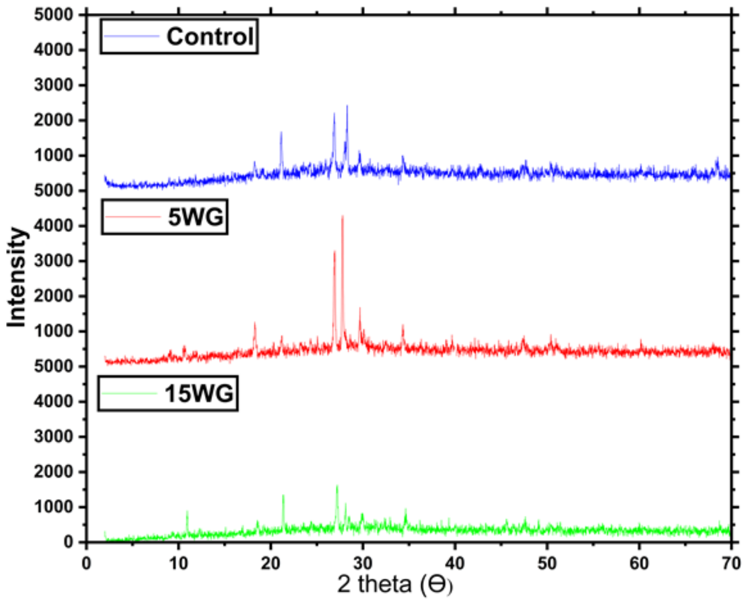

Fig. 17. XRD of various waste glass replacement

The SEM images of the ternary blended hardened concrete are presented in Figs. 19a, 19b, and 19c. Fig. 19b shows the densest microstructure, with well-formed C-S-H gels filling the pores, contributing to the highest strength in the mix after 56 curing days. The ternary blend of 10% WGP and 5% MK (Fig. 19b) promotes additional pozzolanic reactions, enhancing the overall matrix. Fig. 19c (10% MK and 5% WGP) displays a microstructure denser than the control but less so than the 10% WGP and 5% MK blend, with fewer visible C-S-H gels. Some micro cracks and pores remain in the 10% MK and 5% WGP ternary mix, resulting in lower strength compared to the ternary blend of 10% WGP and 5% MK. The XRD graph of the ternary blended hardened concrete is presented in Fig. 20. The 5MK10WG mix revealed a more pronounced hump in the 2θ range of 29°–34°, indicating a higher formation of C-S-H. Additionally, the reduction in the intensity of the portlandite peaks suggests more complete hydration and pozzolanic reaction, which is consistent with the SEM results, correlating with its highest strength. The 10MK5WG mix shows a moderate hump in the 2θ range of 29°–34°, indicating C-S-H formation, but it is less intense than the 5MK10WGP mix. There are also noticeable peaks for unreacted phases, which correlates with the observed lower strength compared to the 5MK10WGP mix.

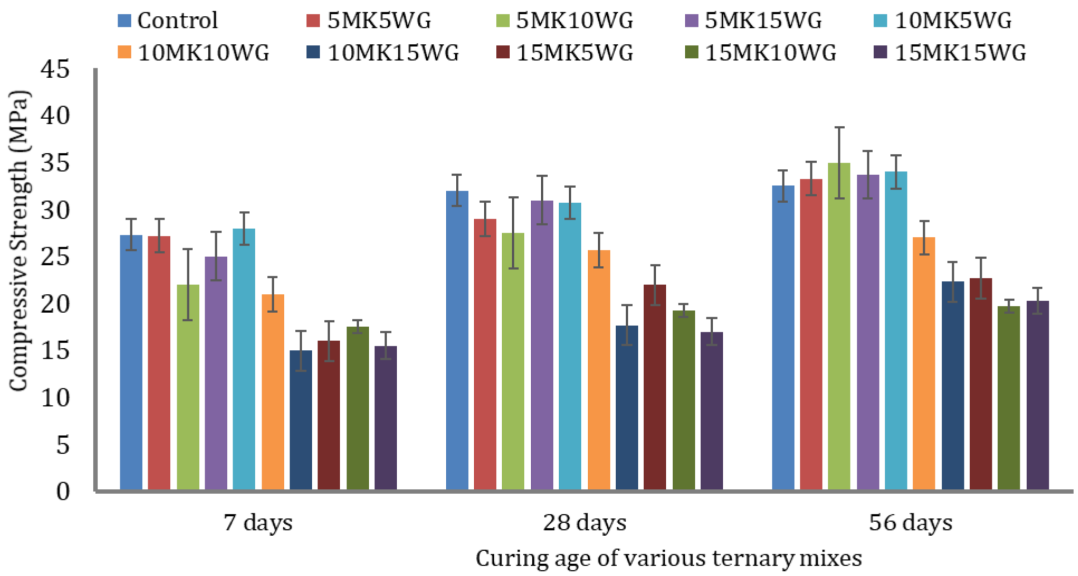

Fig. 18. Compressive strength tests result of ternary blended MK AND WGP with cement

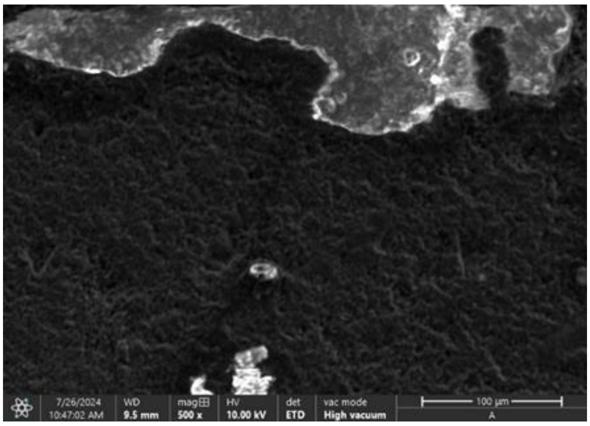

(a)

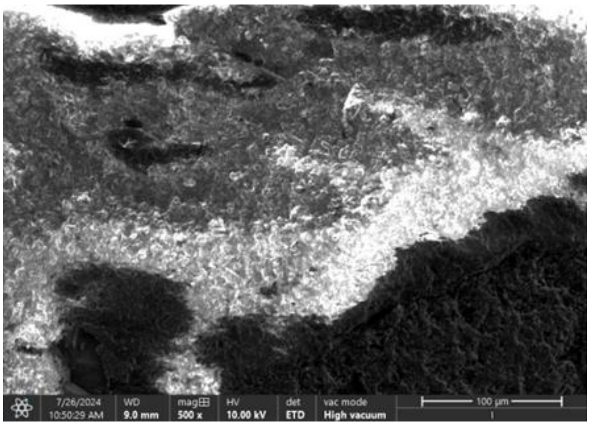

(b)

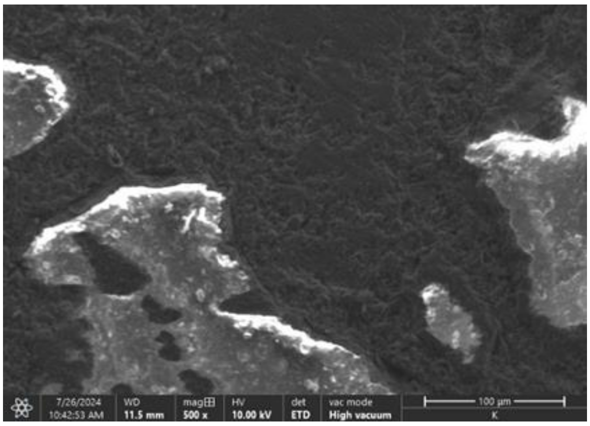

(c)

Fig. 19. (a) SEM image of control (b) SEM image of 5MK10GP, and (c) SEM image of 10MK5WGP

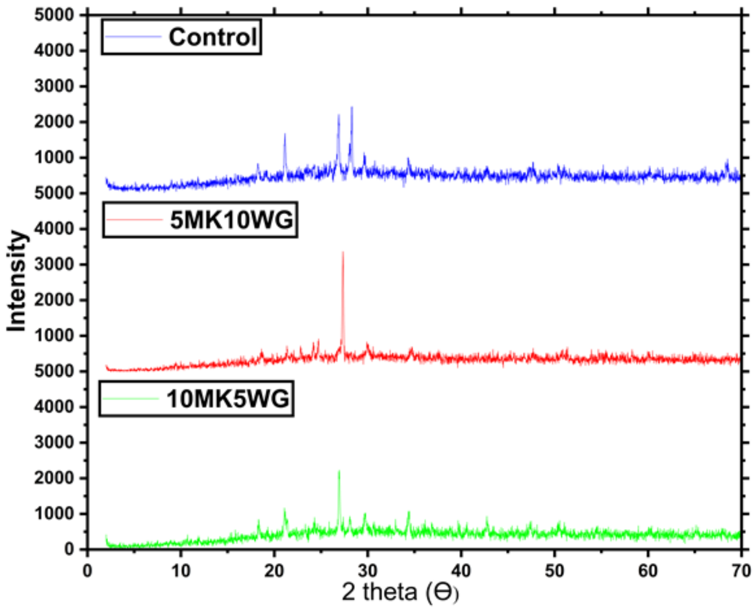

Fig. 20. XRD Graphs of ternary blended mixes

3.4.2 Split Tensile Strength

The experimental results for the split tensile strength of concrete samples containing varying percentages of binary and ternary combinations of MK and WGP with cement are illustrated in Figs. 21, 22, and 23. The results indicate that the split tensile strength improves as the curing duration increases, with all samples showing a consistent increase from 7 days to 56 days. Fig. 21 reveals that the split tensile strength rises with MK replacement up to 15%, beyond which further replacement results in a decline in strength.

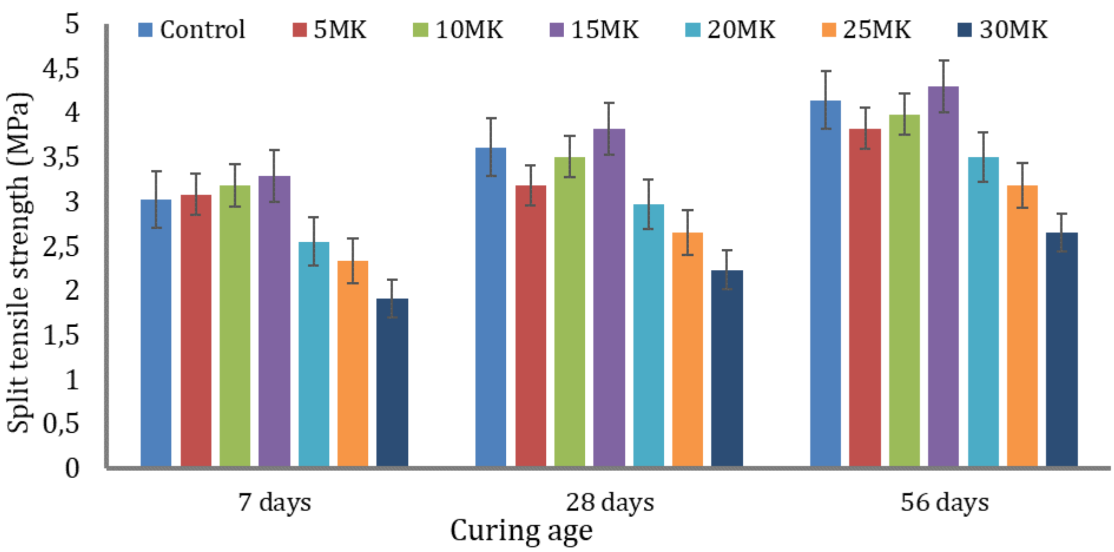

Fig. 21. Split tensile strength tests result of binary blended MK with cement

A similar pattern is evident in Fig. 22, where increasing the waste glass powder (WGP) content enhances the split tensile strength up to a 15% replacement level, after which further replacement results in a decline in strength. This partially aligns with the findings of Shamsudeen et al. [75], who identified 10% as the optimal replacement level of cement with WGP for achieving maximum split tensile strength in their study. Fig. 23 shows that the ternary mix 5MK10WG performs better having the highest split tensile strength compared to the control and other mixes, thus the optimum replacement level for the split tensile strength.

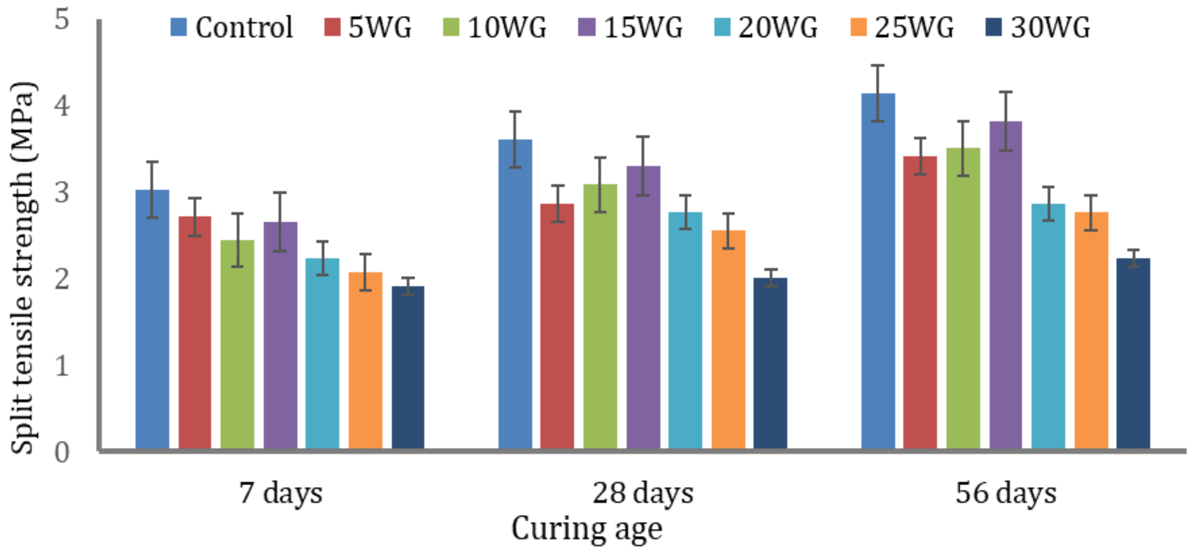

Fig. 22. Split tensile strength tests result of binary blended WGP with cement

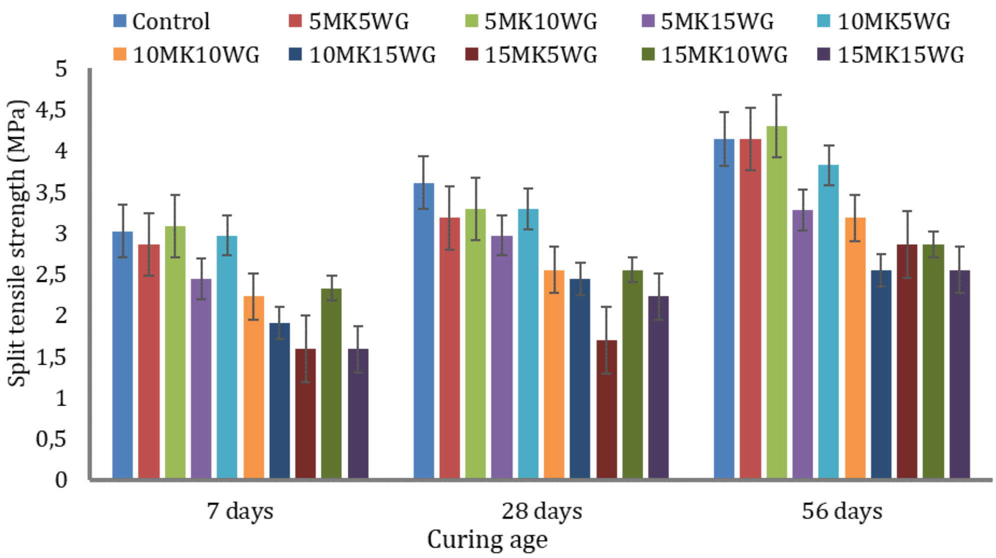

Fig. 23. Split tensile strength tests result of ternary blended MK and WGP with cement

4. Conclusions

In conclusion, the following can be drawn based on the outcomes of this research work

- XRD analysis confirmed that the Metakaolin (MK) and Waste Glass Powder (WGP) particles are predominantly amorphous and can be classified as pozzolan, though the combined Al_2O_3, SiO_2, and Fe_2O_3 content in both materials are slightly below the ASTM C618 recommended threshold.
- The mixtures with WGP exhibited higher slump values and reduced flow time compared to those containing MK, indicating greater workability. This could be attributed to microstructural properties, where MK particles are densely packed with minimal micropores, irregular shapes, rough surfaces, and high surface area, while WGP particles have angular, irregular shapes with smoother surfaces, and are more loosely packed.
- The compressive strength results reveal that 15% replacement is the optimum level for both binary and ternary combinations, with the 5MK10WGP mix achieving the highest compressive strength compared to the control and other mixes at 56 days. This performance could be attributed to enhanced pozzolanic reactions, which facilitated improved C-S-H formation and a reduction in portlandite content. The denser microstructure observed, with

well-formed C-S-H gels filling pores in the 5MK10WGP mix, further validates its superior strength development.

- Although samples with 5MK10WGP was optimum in terms of both compressive and tensile strength after 90days of curing, the mix 5MK15WGP (20% replacement) also demonstrated consistently good performance at both 28 and 90 days as per compressive strength. However, the tensile strength was very low compared to 5MK10WGP samples probably due to the brittle nature of the glass material.
- The split tensile strength results also indicate that 15% replacement is the optimum level for all blended combinations, with the 15MK and 5MK10WGP mixes achieving the highest strength compared to the control at 56 days. This outcome can be linked to enhanced pozzolanic reactions, which improve the bond between aggregates and the cement matrix, as well as the denser microstructures observed in these mixes, resulting in superior tensile strength development.
- Among all the mixes, the ternary mix with 5% MK and 10% WGP (5MK+10WGP) demonstrated superior mechanical properties, surpassing the control mix by 7.7% in compressive strength and 3.8% in split tensile strength after 56 days of curing.

References

[1] Singh H, Siddique R. Long term durability assessment of self-compacting concrete made with crushed recycled glass and metakaolin. Constr Build Mater. 2023 Oct;400:132656. https://doi.org/10.1016/j.conbuildmat.2023.132656

[2] Akinpelu MA, Odeyemi SO, Olafusi OS, Muhammed FZ. Evaluation of splitting tensile and compressive strength relationship of self-compacting concrete. J King Saud Univ Eng Sci. 2019 Jan;31(1):19-25. https://doi.org/10.1016/j.jksues.2017.01.002

[3] Gill AS, Siddique R. Strength and micro-structural properties of self-compacting concrete containing metakaolin and rice husk ash. Constr Build Mater. 2017 Dec;157:51-64. https://doi.org/10.1016/j.conbuildmat.2017.09.088

[4] Sharma R, Khan RA. Durability assessment of self compacting concrete incorporating copper slag as fine aggregates. Constr Build Mater. 2017 Nov;155:617-29. https://doi.org/10.1016/j.conbuildmat.2017.08.074

[5] Silva P, de Brito J. Experimental study of the mechanical properties and shrinkage of self-compacting concrete with binary and ternary mixes of fly ash and limestone filler. Eur J Environ Civ Eng. 2017 Apr;21(4):430-53. https://doi.org/10.1080/19648189.2015.1131200

[6] Mohan A, Mini KM. Strength and durability studies of SCC incorporating silica fume and ultra fine GGBS. Constr Build Mater. 2018 May;171:919-28. https://doi.org/10.1016/j.conbuildmat.2018.03.186

[7] Pathak N, Siddique R. Effects of elevated temperatures on properties of self-compacting-concrete containing fly ash and spent foundry sand. Constr Build Mater. 2012 Sep;34:512-21. https://doi.org/10.1016/j.conbuildmat.2012.02.026

[8] Bingöl AF, Tohumcu I. Effects of different curing regimes on the compressive strength properties of self compacting concrete incorporating fly ash and silica fume. Mater Des. 2013 Oct;51:12-8. https://doi.org/10.1016/j.matdes.2013.03.106

[9] Avğın S, Köse MM, Özbek A. Damage assessment of structural and geotechnical damages in Kahramanmaraş during the February 6, 2023 earthquakes. Eng Sci Technol Int J. 2024 Sep;57:101811. https://doi.org/10.1016/j.jestch.2024.101811

[10] Isik E, Harirchian E, Bilgin H, Jadhav K. The effect of material strength and discontinuity in RC structures according to different site-specific design spectra. Res Eng Struct Mater. 2020 May;7(3):413-30.

[11] Zengin B, Aydin F. The effect of material quality on buildings moderately and heavily damaged by the Kahramanmaraş earthquakes. Appl Sci. 2023 Sep;13(19):10668. https://doi.org/10.3390/app131910668

[12] Işık E, Harirchian E, Bilgin H, Jadhav K. Seismic performance and failure mechanisms of reinforced concrete structures subject to the earthquakes in Türkiye. Sustainability. 2024 Jul;16(15):6473. https://doi.org/10.3390/su16156473

[13] Tomar R, Kishore K, Singh Parihar H, Gupta N. A comprehensive study of waste coconut shell aggregate as raw material in concrete. Mater Today Proc. 2021 Jan;44:437-43. https://doi.org/10.1016/j.matpr.2020.09.754

[14] Kishore K, Gupta N. Mechanical characterization and assessment of composite geopolymer concrete. Mater Today Proc. 2021 Jan;44:58-62. https://doi.org/10.1016/j.matpr.2020.06.319

[15] Rodrigues FA, Joekes I. Cement industry: Sustainability, challenges and perspectives. Environ Chem Lett. 2011 Oct;9(2):151-66. https://doi.org/10.1007/s10311-010-0302-2

[16] Zhang J, Liu G, Chen B, Song D, Qi J, Liu X. Analysis of CO2 emission for the cement manufacturing with alternative raw materials: A LCA-based framework. Energy Procedia. 2014 Jan;61:2541-5. https://doi.org/10.1016/j.egypro.2014.12.041

[17] Shukla A, Gupta N, Gupta A. Development of green concrete using waste marble dust. Mater Today Proc. 2020 Jan;26:2590-4. https://doi.org/10.1016/j.matpr.2020.02.548

[18] Thapa VB, Waldmann D, Simon C. Gravel wash mud, a quarry waste material as supplementary cementitious material (SCM). Cem Concr Res. 2019 Oct;124:105833. https://doi.org/10.1016/j.cemconres.2019.105833

[19] Muralidharan R, Park T, Yang HM, Lee SY, Subbiah K, Lee HS. Review of the effects of supplementary cementitious materials and chemical additives on the physical, mechanical and durability properties of hydraulic concrete. Materials. 2021 Dec;14(23):7270. https://doi.org/10.3390/ma14237270

[20] Hakeem IY, Amin M, Agwa IS, Rizk MS, Abdelmagied MF. Effect of using sugarcane leaf ash and granite dust as partial replacements for cement on characteristics of ultra-high performance concrete. Case Stud Constr Mater. 2023 Dec;19:e02266. https://doi.org/10.1016/j.cscm.2023.e02266

[21] Hakeem IY, Amin M, Agwa IS, Abd-Elrahman MH, Ibrahim OMO, Samy M. Ultra-high-performance concrete properties containing rice straw ash and nano eggshell powder. Case Stud Constr Mater. 2023 Dec;19:e02291. https://doi.org/10.1016/j.cscm.2023.e02291

[22] Ahmed MM, Sadoon A, Bassuoni MT, Ghazy A. Utilizing agricultural residues from hot and cold climates as sustainable SCMs for low-carbon concrete. Sustainability. 2024 Dec;16(23):10715. https://doi.org/10.3390/su162310715

[23] Statista. Glass recycling facts globally 2018 | Statista [Internet]. [cited 2024 Nov 14]. Available from: https://www.statista.com/statistics/1055604/key-figures-glass-recycling-globally/

[24] UNIDO. Industrial Development Report 2020 [Internet]. United Nations Industrial Development Organization; 2020 [cited 2024 Nov 14]. Available from: https://www.unido.org/resources-publications-industrial-development-report-series/idr2020

[25] Federico LM, Chidiac SE. Waste glass as a supplementary cementitious material in concrete - Critical review of treatment methods. Cem Concr Compos. 2009 Sep;31(8):606-10. https://doi.org/10.1016/j.cemconcomp.2009.02.001

[26] Kashani A, Ngo TD, Hajimohammadi A. Effect of recycled glass fines on mechanical and durability properties of concrete foam in comparison with traditional cementitious fines. Cem Concr Compos. 2019 May;99:120-9. https://doi.org/10.1016/j.cemconcomp.2019.03.004

[27] Taha B, Nounu G. Utilizing waste recycled glass as sand/cement replacement in concrete. J Mater Civ Eng. 2009 Nov;21(12):709-21. https://doi.org/10.1061/(ASCE)0899-1561(2009)21:12(709)

[28] Arabi N, Meftah H, Amara H, Kebaïli O, Berredjem L. Valorization of recycled materials in development of self-compacting concrete: Mixing recycled concrete aggregates - Windshield waste glass aggregates. Constr Build Mater. 2019 Jun;209:364-76. https://doi.org/10.1016/j.conbuildmat.2019.03.024

[29] Guo P, Meng W, Nassif H, Gou H, Bao Y. New perspectives on recycling waste glass in manufacturing concrete for sustainable civil infrastructure. Constr Build Mater. 2020 Oct;257:119579. https://doi.org/10.1016/j.conbuildmat.2020.119579

[30] Hendi A, Mostofinejad D, Sedaghatdoost A, Zohrabi M, Naeimi N, Tavakolinia A. Mix design of the green self-consolidating concrete: Incorporating the waste glass powder. Constr Build Mater. 2019 Feb;199:369-84. https://doi.org/10.1016/j.conbuildmat.2018.12.020

[31] ouldkhaoua Y, Benabed B, Abousnina R, Kadri EH. Experimental study on the reuse of cathode ray tubes funnel glass as fine aggregate for developing an ecological self-compacting mortar incorporating metakaolin. J Build Eng. 2020 Jan;27:100951. https://doi.org/10.1016/j.jobe.2019.100951

[32] Singh H, Siddique R. Utilization of crushed recycled glass and metakaolin for development of self-compacting concrete. Constr Build Mater. 2022 Sep;348:128659. https://doi.org/10.1016/j.conbuildmat.2022.128659

[33] Solanki P, Xie H. State-of-the-practice review on the field-curing methods for evaluating strength of concrete test specimen. J Civ Eng Constr. 2022 Aug;11(3):153-65. https://doi.org/10.32732/jcec.2022.11.3.153

[34] Bisht K, Kabeer KISA, Ramana PV. Gainful utilization of waste glass for production of sulphuric acid resistance concrete. Constr Build Mater. 2020 Feb;235:117486. https://doi.org/10.1016/j.conbuildmat.2019.117486

[35] Tanwar V, Bisht K, Kabeer KISA, Ramana PV. Experimental investigation of mechanical properties and resistance to acid and sulphate attack of GGBS based concrete mixes with beverage glass waste as fine aggregate. J Build Eng. 2021 Sep;41:102372. https://doi.org/10.1016/j.jobe.2021.102372

[36] Adaway M, Wang Y. Recycled glass as a partial replacement for fine aggregate in structural concrete - Effects on compressive strength. Electron J Struct Eng. 2015 Jan;14(1):116-22. https://doi.org/10.56748/ejse.141951
[37] Malik MI, Bashir M, Ahmad S, Tariq T, Chowdhary U. Study of concrete involving use of waste glass as partial replacement of fine aggregates [Internet]. 2013 [cited 2024 Nov 14]. Available from: www.iosrjen.org
[38] Rashad AM. Recycled waste glass as fine aggregate replacement in cementitious materials based on Portland cement. Constr Build Mater. 2014 Dec;72:340-57. https://doi.org/10.1016/j.conbuildmat.2014.08.092
[39] Tamanna N, Tuladhar R, Sivakugan N. Performance of recycled waste glass sand as partial replacement of sand in concrete. Constr Build Mater. 2020 Apr;239:117804. https://doi.org/10.1016/j.conbuildmat.2019.117804
[40] Tan KH, Du H. Use of waste glass as sand in mortar: Part I - Fresh, mechanical and durability properties. Cem Concr Compos. 2013 Jan;35(1):109-17. https://doi.org/10.1016/j.cemconcomp.2012.08.028
[41] Luo D, Sinha A, Adhikari M, Wei J. Mitigating alkali-silica reaction through metakaolin-based internal conditioning: New insights into property evolution and mitigation mechanism. Cem Concr Res. 2022 Sep;159:106888. https://doi.org/10.1016/j.cemconres.2022.106888
[42] Akinpelu MA, Salman A-SM, Jimoh YA, Yahaya IT, Salami HM. Impact of treatment temperature of metakaolin on strength and sulfate resistance of concrete. Res Eng Struct Mater. 2024.
[43] Bernal SA, et al. Characterization of supplementary cementitious materials by thermal analysis. Mater Struct. 2017 Feb;50(1):1-13. https://doi.org/10.1617/s11527-016-0909-2
[44] Cao Z, Shen L, Liu L, Zhong S. Analysis on major drivers of cement consumption during the urbanization process in China. J Clean Prod. 2016 Oct;133:304-13. https://doi.org/10.1016/j.jclepro.2016.05.130
[45] Rashad AM. Recycled waste glass as fine aggregate replacement in cementitious materials based on Portland cement. Constr Build Mater. 2014 Dec;72:340-57. https://doi.org/10.1016/j.conbuildmat.2014.08.092
[46] Ling G, et al. Rheological behavior and microstructure characteristics of SCC incorporating metakaolin and silica fume. Materials. 2018 Dec;11(12):2576. https://doi.org/10.3390/ma11122576
[47] Sfikas IP, Badogiannis EG, Trezos KG. Rheology and mechanical characteristics of self-compacting concrete mixtures containing metakaolin. Constr Build Mater. 2014 Aug;64:121-9. https://doi.org/10.1016/j.conbuildmat.2014.04.048
[48] Boukendakdji O, Kadri EH, Kenai S. Effects of granulated blast furnace slag and superplasticizer type on the fresh properties and compressive strength of self-compacting concrete. Cem Concr Compos. 2012 Apr;34(4):583-90. https://doi.org/10.1016/j.cemconcomp.2011.08.013
[49] Letelier V, Henríquez-Jara BI, Manosalva M, Parodi C, Ortega JM. Use of waste glass as a replacement for raw materials in mortars with a lower environmental impact. Energies. 2019 May;12(10):1974. https://doi.org/10.3390/en12101974
[50] Younes MM, Abdel-Rahman HA, Khattab MM. Utilization of rice husk ash and waste glass in the production of ternary blended cement mortar composites. J Build Eng. 2018 Nov;20:42-50. https://doi.org/10.1016/j.jobe.2018.07.001
[51] Keerio MA, Abbasi SA, Kumar A, Bheel N, Rehaman KU, Tashfeen M. Effect of silica fume as cementitious material and waste glass as fine aggregate replacement constituent on selected properties of concrete. Silicon. 2022 Jan;14(1):165-76. https://doi.org/10.1007/s12633-020-00806-6
[52] Shoaei P, Ameri F, Musaeei HR, Ghasemi T, Cheah CB. Glass powder as a partial precursor in Portland cement and alkali-activated slag mortar: A comprehensive comparative study. Constr Build Mater. 2020 Aug;251:118991. https://doi.org/10.1016/j.conbuildmat.2020.118991
[53] Figueira RB, et al. Alkali-silica reaction in concrete: Mechanisms, mitigation and test methods. Constr Build Mater. 2019 Oct;222:903-31. https://doi.org/10.1016/j.conbuildmat.2019.07.230
[54] Saha AK, Khan MNN, Sarker PK, Shaikh FA, Pramanik A. The ASR mechanism of reactive aggregates in concrete and its mitigation by fly ash: A critical review. Constr Build Mater. 2018 May;171:743-58. https://doi.org/10.1016/j.conbuildmat.2018.03.183
[55] British Standards Institution. BS EN 197-1:2011 Cement - Part 1: Composition, specifications and conformity criteria. London: BSI; 2011.
[56] British Standards Institution. BS EN 12620: Aggregates for concrete. London: BSI; 2008.
[57] British Standards Institution. BS EN 1008: Mixing water for concrete - Specification for sampling, testing and assessing the suitability of water. London: BSI; 2002.
[58] British Standards Institution. BS EN 1097-6: Tests for mechanical and physical properties of aggregates - Part 6: Determination of particle density and water absorption. London: BSI; 2022.
[59] EFNARC. The European Guidelines for Self-Compacting Concrete - Specification, Production and Use. 2005. [Online]. Available: www.efnarc.org

[60] EFNARC. Specification and Guidelines for Self-Compacting Concrete. 2002. [Online]. Available: www.efnarc.org
[61] British Standards Institution. BS EN 12350-2: Testing fresh concrete - Slump test. London: BSI; 2019. [Online]. Available: https://www.en-standard.eu/bs-en-12350-2-2019-testing-fresh-concrete-slump-test/
[62] British Standards Institution. BS EN 12350-9: Testing fresh concrete - Part 9: Self-compacting concrete - V-funnel test. London: BSI; 2010.
[63] British Standards Institution. BS EN 12350-10: Testing fresh concrete - Part 10: Self-compacting concrete - L-box test. London: BSI; 2010.
[64] British Standards Institution. BS EN 12390-3:2019: Testing hardened concrete - Compressive strength of test specimens. London: BSI; 2019. [Online]. Available: https://www.en-standard.eu/bs-en-12390-3-2019-testing-hardened-concrete-compressive-strength-of-test-specimens/
[65] British Standards Institution. BS EN 12390-6:2023: Testing hardened concrete - Split tensile strength test. London: BSI; 2023. [Online]. Available: https://knowledge.bsigroup.com
[66] ASTM International. ASTM C1602/C1602M: Standard Specification for Mixing Water Used in the Production of Hydraulic Cement Concrete. USA: ASTM; 2018.
[67] Salman AM, Akinpelu MA, Yahaya IT, Salami HM. Workability and strengths of ternary cementitious concrete incorporating calcined clay and limestone powder. Mater Today Proc. 2023 Jan;86:51-8. https://doi.org/10.1016/j.matpr.2023.02.249
[68] ASTM International. ASTM C618-23e1: Standard Specification for Coal Fly Ash and Raw or Calcined Natural Pozzolan for Use in Concrete. [Online]. Available: https://webstore.ansi.org/standards/astm/astmc61812a
[69] Guignone GC, Vieira GL, Zulcão R, Degen MK, de Moraes Mittri SH, Baptista G. Incorporation of glass powder and metakaolin as cement partial replacement to improve concrete mechanical properties and increase service life. J Compos Mater. 2020 Feb;54(21):2965-83. https://doi.org/10.1177/0021998320906873
[70] Chavali BT, Karunakar P, Tech M. Effect of varying quantities of metakaolin and fly ash on strength characteristics of concrete [Internet]. 2016. Available from: www.ijtre.com
[71] Ofuyatan OM, Olowofoyeku AM, Edeki SO, Oluwafemi J, Ajao A, David O. Incorporation of silica fume and metakaolin on self-compacting concrete. J Phys Conf Ser. 2019 Dec;1378(4):042089. https://doi.org/10.1088/1742-6596/1378/4/042089
[72] Lekhya A, Kumar NS. A study on the effective utilization of ultrafine fly ash and silica fume content in high-performance concrete through an experimental approach. Heliyon. 2024 Nov;10(22). https://doi.org/10.1016/j.heliyon.2024.e39678
[73] Alamri M, et al. Enhancing the engineering characteristics of sustainable recycled aggregate concrete using fly ash, metakaolin and silica fume. Heliyon. 2024 Apr;10(7):29014. https://doi.org/10.1016/j.heliyon.2024.e29014
[74] Fonchou WAD, Abanda A, Kenmogne F, Sali M, Doumbaye JM. Partial replacement of cement with waste glass powder in concrete for sustainable waste management: A case study of concrete incorporating sand and waste glass from the Douala City of Cameroon. Am J Mater Sci. 2023;13(1):7-21.
[75] Shamsudeen AA, Usman N, Idi MA, Gabriel U. Suitability of waste glass powder as partial cement replacement in concrete subject to chemical aggressive environment [Internet]. 2020. Available from: www.ijltemas.in
[76] Elyasigorji F, et al. Comprehensive review of direct and indirect pozzolanic reactivity testing methods. Buildings. 2023 Nov;13(11):2789. https://doi.org/10.3390/buildings13112789